

Serum-derived exosomes containing NEAT1 promote the occurrence of rheumatoid arthritis through regulation of miR-144-3p/ROCK2 axis

Rui Liu*, Chunbo Jiang*, Jingjing Li, Xiaoru Li, Lin Zhao, Haifeng Yun, Weiwei Xu, Weijian Fan, QiuHong Liu^{ID} and Hongli Dong

Abstract

Background: Evidence has demonstrated that non-coding RNAs (ncRNAs) could be delivered efficiently to recipient cells using exosomes as a carrier. Additionally, long ncRNA nuclear enriched abundant transcript 1 (NEAT1) is emerging as a vital regulatory molecule in the progression of rheumatoid arthritis (RA). The aim of this study was to identify the NEAT1/miR-144-3p/Rho-associated protein kinase 2 (ROCK2) functional network regulating the WNT signaling pathway in RA.

Methods: *In vivo*, a collagen-induced arthritis (CIA) model was established to analyze the effects of blood exosomes on the incidence, clinical score, and bone degradation of RA. *In vitro*, the CD4⁺T cells were characterized by flow cytometry and the cell activities were analyzed in the presence of exosome treatment alone or in combination with altered expression of NEAT1, miR-144-3p or Rho-associated protein kinase 2 (ROCK2). The expression of NEAT1, miR-144-3p, ROCK2, and corresponding proteins in the WNT signaling pathway was detected by RT-qPCR and western blot techniques. The binding profile of NEAT1 to miR-144-3p was evaluated *via* a combination approach of luciferase activity assay, RNA immunoprecipitation, and RNA pull-down experiments.

Results: Blood exosomes extracted from RA patients increased the incidence of RA and bone destruction significantly. Overexpression of NEAT1 or ROCK2 promoted immune cell (CD4⁺T cells) proliferation, Th17 cell differentiation, and cell migration in response to stimulus, whereas knockout of the NEAT1 gene induced the expression of miR-144-3p in CD4⁺T cells. ROCK2 exogenous expression inhibited the expression of miR-144-3p, inducing activation of the WNT signaling pathway.

Conclusion: A novel regulatory pathway NEAT1/miR-144-3p/ROCK2/WNT in RA was investigated as a potential target for RA therapy.

Keywords: exosomes, miR-144-3p, NEAT1, rheumatoid arthritis, ROCK2, WNT signaling pathway

Received: 10 August 2020; revised manuscript accepted: 12 January 2021.

Introduction

Rheumatoid arthritis (RA), one of the more common autoimmune disorders, affects 0.5–1% of the population, with up to 50 cases per 100,000 people.^{1,2} RA is characterized by chronic joint inflammation, leading to cartilage and bone damage as well as disability.^{3,4} Increased mortality

remains a challenge worldwide.⁵ The keys to optimal therapeutic success are early diagnosis and treatment, including the use of biologic disease-modifying anti-rheumatic drugs, leading to long-term drug-free remission.⁶ Up to 50% of RA is attributed to genetic factors.^{7,8} Environmental factors, including cigarette smoking, are also risk

Ther Adv Chronic Dis

2021, Vol. 12: 1–17

DOI: 10.1177/
20406223211991705

© The Author(s), 2021.
Article reuse guidelines:
sagepub.com/journals-
permissions

Correspondence to:

QiuHong Liu
Department of
Rheumatology, Suzhou
TCM Hospital Affiliated
to Nanjing University of
Chinese Medicine, No. 18,
Yangsu Road, Gusu District,
Suzhou, Jiangsu Province
215009, P.R. China
liuqiuHongSuzhou@163.com

Hongli Dong
Department of
Encephalopathy, Suzhou
TCM Hospital Affiliated
to Nanjing University of
Chinese Medicine, No. 18,
Yangsu Road, Gusu District,
Suzhou, Jiangsu Province
215009, P.R. China
dhl218@163.com

Rui Liu
Jingjing Li
Xiaoru Li
Lin Zhao
Weiwei Xu
Department of
Rheumatology, Suzhou
TCM Hospital Affiliated
to Nanjing University of
Chinese Medicine, Suzhou,
P.R. China

Chunbo Jiang
Department of Nephrology,
Suzhou TCM Hospital
Affiliated to Nanjing
University of Chinese
Medicine, Suzhou, P.R.
China

Haifeng Yun
Department of Internal
Medicine, Suzhou TCM
Hospital Affiliated to
Nanjing University of
Chinese Medicine, Suzhou,
P.R. China

Weijian Fan
Department of Vascular
Surgery, Suzhou TCM
Hospital Affiliated to
Nanjing University of
Chinese Medicine, Suzhou,
P.R. China

*Joint first authors

factors for RA.^{7,9} However, the exact risk factors and molecular mechanisms for the pathogenesis of RA remain incompletely understood. In our investigation, mechanisms underlying RA progresses were determined. In the pathological process of RA, CD4⁺T lymphocytes account for a large proportion of inflammatory cells.¹⁰ The differentiation of CD4⁺T cells to Th17 cells is critical for the progression of RA.^{11,12}

Recent studies have shown that the functions of extracellular vesicles are diverse, and include intercellular communication through the transmission of proteins, mRNA, miRNA, and long non-coding RNAs (lncRNAs).^{13,14} Evidence has demonstrated that the exosomes of stressed peripheral blood mononuclear cells (PBMCs) were capable of promoting wound healing and angiogenesis *in vitro* and *in vivo*.¹⁵ Considering the pathological relevance of RA and the delivery of molecules at a distance beyond direct cell-to-cell contact, we decided to analyze lncRNAs in serum exosomes. A previous report showed that the expression of nuclear enriched abundant transcript 1 (NEAT1) is increased in blood from RA patients.¹⁶ Moreover, high expression of ncRNAs Hotair and NEAT1 was found in PBMCs and serum exosome of RA patients, leading to the migration of active macrophages.¹⁶ NEAT1 was found to be poorly expressed in activated CD4⁺T cells.¹⁷ However, there are few studies on the involvement of NEAT1 in the differentiation of CD4⁺T cells into Th17 cells.

miR-144-3p is a microRNA that is linked to RA.¹⁸ More importantly, although not related to RA, NEAT1 has been shown previously to bind miR-144-3p.¹⁹ In the current study, we determined whether miR-144-3p could be a downstream signaling mediator in RA. Furthermore, miR-144-3p negatively regulates the expression of Rho-associated protein kinase 2 (ROCK2) in osteosarcoma.²⁰ ROCK2 is involved in immune defense, inflammation, and RA.^{21,22} In particular, ROCK2 has critical roles in different biological processes by activating Wnt/ β -catenin.²³ Moreover, Wnt/ β -catenin plays a critical role in inflammation.²⁴ In addition, the Wnt/ β -catenin signaling pathway has also been linked to RA.²⁵ Wnt/ β -catenin inhibition was shown to alleviate RA.²⁶

In light of previous studies, we determined the impact of serum-derived exosome containing NEAT1 in RA through regulation of the miR-144-3p/ROCK2/Wnt/ β -catenin axis.

Methods

Ethics statement

All study participants signed informed consent to provide peripheral blood for the study. The research was approved by the Ethics committee of Suzhou TCM Hospital Affiliated to Nanjing University of Chinese Medicine and all operations were in compliance with the Declaration of Helsinki. The All animal experiments were performed with the approval of the institutional animal care and use committee of Suzhou TCM Hospital Affiliated to Nanjing University of Chinese Medicine.

Study subjects

The 2010 ACR/EULAR classification criteria were used to diagnose patients with RA.²⁷ RA patients from Suzhou TCM Hospital Affiliated to Nanjing University of Chinese Medicine between May 2014 and May 2018 were selected for experiment. Inclusion criteria: aged ≥ 18 years; at least two joints swelling; symptoms lasting for less than 6 months. Exclusion criteria: patients who had taken any anti-rheumatic drugs that improved their condition before entering the study; presence of ankylosing spondylitis, infectious arthritis, systemic lupus erythematosus, and other inflammatory diseases. The demographics of RA patients who had not received any treatment in the past and healthy volunteers are listed in Table 1. Blood samples were drawn into a vacuum tube (Venoject II, VPAS109K50; Terumo Corporation, Tokyo, Japan), centrifuged at $1500 \times g$ for 10 min, and the serum was separated at room temperature. The separated serum samples were then stored at -80°C until use.

Isolation and evaluation of exosomes

Exosomes were isolated from serum using an exosome extraction kit (Cell Guidance Systems, Cambridge, UK).²⁴ Briefly, the serum sample was centrifuged at $1200 \times g$ for 15 min, $2000 \times g$ for 20 min, and $10,000 \times g$ for 45 min, and the final supernatant was collected. The supernatant was mixed with polyethylene glycol (PEG) buffer (30% PEG 6000, 50 mmol/l HEPES, 1 mol/l NaCl) at a volume ratio of 5: 1. Exosomes isolated and resuspend in phosphate buffer saline (PBS) after the mixture were centrifuged at $10,000 \times g$ for 30 min.

Table 1. Clinical features of RA patients.

Variables	HC	RA
Number of patients	20	68
Age (years), median (range)	51.9; 31–72	54.8; 28–83
Sex (male/female)	5/15	12/56
Disease duration (years), mean (range)	–	6.9 (1–20)
SJC, mean (range)	–	6 (3–10)
TJC, mean (range)	–	7 (2–13)
DAS28-ESR, mean (range)	–	5.2 (3.9–6.1)
DAS28-CRP, mean (range)	–	4.1 (2.9–4.7)
ESR (mm/h), mean (range)	9.8 (4–15)	38 (23–60)
RF (positive/negative)	–	59/9
CRP (median; range) (mg/dl)	0.9; 0.3–1.7	3.3; 0.2–9.1
Krenn's score		
4	–	5
5	–	5
6	–	13
7	–	19
8	–	16
9	–	10

CRP, C-reactive protein; DAS28-CRP, disease activity score 28 joints using C-reactive protein; DAS28-ESR, disease activity score 28 joints using erythrocyte sedimentation rate; ESR, erythrocyte sedimentation rate; HC, healthy controls; RA, rheumatoid arthritis; RF, rheumatoid factor; SJC, swollen joint count; TJC, tender joint count.

Size distribution of exosomes was determined by nanoparticle tracking analysis (NTA) using a NanoSight LM10-12 instrument (NTA 3.1 build 3.1.54; Malvern Instruments, Orsay, France) with the following parameters: camera level 13; threshold 5; 22.4°C; three videos per analyzed sample. The topography of exosomes was scanned by transmission electron microscope (TEM, Morgagni 268D, Philips, Holland).¹⁶ Briefly, the exosomes were fixed in 3% (w/v) glutaraldehyde and 2% paraformaldehyde buffer, and then loaded into a Formvar-coated copper mesh. The copper mesh was washed, placed in a 2% uranyl acetate solution, and then dried on gilder grids for further use. The surface markers of exosome, CD63 (ab134045, 1:1000, Abcam, Cambridge, UK) and CD9 (ab92726, 1:2000, Abcam), were analyzed by western blot.

Collagen-induced arthritis model

Nine-week-old DBA/1J mice were induced to develop arthritis.²⁸ Briefly, bovine collagen type II (bCII, 2 mg/ml, c7806, Sigma) was diluted in acetic acid (0.05 M) and emulsified with Freund's complete adjuvant (Thermoscientific, Rockford, IL, USA). Before the experiment, mice were anesthetized by intravenous injection of pentobarbital sodium (25 mg/kg). On the first day, 100 µl of emulsion was injected intradermally into the base of the mouse's tail. On the 21st day, mice were immunized with bCII in Freund's incomplete adjuvant. On the 21st day, the emulsion was prepared and applied as before with the exception of the incomplete adjuvant that was used for boosting arthritis. To testify the efficacy of RA-exosomes, exosomes dissolved in 50 µl PBS (10×10^8) or 50 µl PBS solution were then injected intravenously on days 18

and 24, respectively. To investigate the effect of NEAT1, shRNA targeting NEAT1 or shRNA negative control (NC) was administered intravenously to CIA mice after a booster injection of bCII. Mice in the control group were emulsified with Freund's complete adjuvant and an equal volume of acetic acid and then immunized according to the above method and boosted on day 21. The clinical symptoms of arthritis among mice were scored and recorded: 0 points, no signs of erythema and swelling; 1 point, erythema and mild swelling confined to the tarsal or ankle joint; 2 points, erythema and mild from the ankle joint to the tarsal swelling; 3 points, erythema and moderate swelling from the ankle joint to the metatarsal joint; 4 points, erythema and severe swelling surrounding the ankles, feet and fingers, or rigid limbs. On day 37, mice were euthanized with 3% carbon dioxide, and their hind limbs were fixed in 4% formaldehyde for analysis of bone by X-ray microcomputer computed tomography (μ CT). Joint tissues were collected for subsequent experiments. The working parameter was set up as follows: 50 kV, 500 μ A, 0.5 mm aluminum filter, 180°. The final scans were reconstructed by NRecon software (Bruker, Billerica, MA, USA) and the degree of degradation and thickness of the ankle wedge bone was quantified by CTAn software (Bruker).

Cell isolation and culture

Human peripheral blood was collected from healthy participants. Ficoll-Hypaque density gradient centrifugation was used to prepare PBMCs.²⁹ CD4⁺T cells were isolated from PBMC by human CD4⁺T cell isolation (130-091-301, Miltenyi Biotec, Bergisch Gladbach, Germany). CD4⁺T cells were cultured in Roswell Park Memorial Institute (RPMI) 1640 medium (C11875500BT, Gibco, Brooklyn, NY, USA) containing 100 U/ml penicillin, 100 μ g/ml streptomycin, 0.05 mM non-essential amino acids, 2 mM l-glutamine, and 10% heat-inactivated fetal calf serum (10099141, Gibco) and incubated at 37°C.

Cell transfection

DNA sequence for NEAT1, ROCK2 and their negative control, small hairpin RNAs (shRNAs), were designed and synthesized. They were then amplified by PCR and cloned into the shRNA vector U6/GFP/Neo plasmid (GenePharma, Shanghai, China). The plasmids that were overexpressed with ROCK2 and NEAT1 (pcDNA3.1-ROCK2) were

purchased from Genescreen Biotechnology (Shanghai, China). miR-144-3p mimic and its inhibitor were obtained from Sangon (Shanghai, China). Plasmids and oligonucleotides were transfected using the Lipofectamine™ 2000 transfection reagent (Thermo Fisher Scientific, Waltham, MA, USA) according to the manufacturer's instructions. Briefly, 0.2 μ g of indicator plasmid and 0.4 μ l of liposome 3000 (Thermo Fisher Scientific) were mixed with 5 μ l of Opti-MEM medium (Thermo Fisher Scientific), and the solution were transfected into CD4⁺T or Th17 cells (1×10^7 cells/ml) with a density of 70%. After 48h, the transfection efficiency was detected by reverse transcription-quantitative polymerase chain reaction (RT-qPCR) or western blot.

Cell proliferation and apoptosis analysis

Based on previous work, we conducted cell proliferation and an apoptosis assay.²⁹ CD4⁺T cells transfected with plasmids or treated with exosomes for 5 days were stained with 5 mM 5(6)-carboxyfluorescein diacetate succinimidyl ester (CFSE) (MedChemExpress, Monmouth Junction, NJ, USA) to form fluorescent cells (1×10^7 cells/ml). All cells were incubated with 1 mg/ml of anti-CD3 monoclonal antibodies (1:200, ab135372, Abcam) at 37°C and 1 mg/ml of anti-CD28 monoclonal antibodies (1:1000, ab85986, Abcam) and coated in a 96-well plate at 4°C overnight for further use. Cell proliferation was analyzed using an Accuri C6 flow cytometer (Accuri Cytometers, Ann Arbor, MI, USA).

CD4⁺T cells (1×10^4 cells/ml) were transfected with plasmids or treated with exosomes for 5 days after 18h of incubation with 1ml of culture medium. CD4⁺T cells were then stained with Annexin V-FITC and 5 μ g/ml of propidium iodide (Sigma-Aldrich, Madrid, Spain) in the dark for 15min. All cells were collected and processed by flow cytometry (Becton-Dickinson, Franklin Lakes, NJ, USA) to analyze cell apoptosis.

Th17 cell differentiation

CD4⁺T cells (1×10^6 cells/ml) were cultured with anti-CD3 (1 mg/ml)/anti-CD28 (2 mg/ml) and then 3 ng/ml TGF- β (Peprotech), 40 ng/ml IL-6 (Peprotech), and 30 ng/ml IL-23 (Peprotech) were added into the culture system for 72h to induce Th17 differentiation. Phytohemagglutinin (PMA), ionomycin, and protein transport

inhibitor (GolgiStop, BD Pharmingen, San Diego, CA, USA) were added before the cells were collected and stained. Intracellular IL-17 (2.5 µg/10⁶ cells, RB01, R&D Systems, Minneapolis, MN, USA) staining was either performed after fixation or a permeability buffer treatment, and then detected by flow cytometry. The gating strategy to identify CD4⁺IL-17⁺T cells was as follows. Initial gating was through typical forward and lateral scatter, and CD4⁺T lymphocytes were identified as CD4⁺ expression. Among CD4⁺T cell populations, the highly expressed IL-A subpopulation of IL-17 cells was identified as CD4⁺IL-17⁺T cells. An isotype-matched control antibody was used to establish a positive threshold for each marker.

Transwell migration analysis

Cell migration assays were performed using Transwell chambers (Boyden Chambers, Corning, Cambridge, MA, USA). After Th17 cell digestion terminated, the culture medium was discarded after centrifugation followed by washing 1–2 times with PBS. Cells were then resuspended in a serum-free medium containing bovine serum albumin (BSA) and adjusted to the density of 5 × 10⁵ cells/ml; 200 µl of Th17 cell suspension was added to the Transwell upper chamber while 600 µl of RPMI medium containing 10% fetal bovine serum and CCL20 or exosomes was added to the lower chamber of Transwell. The upper chamber cells were wiped with a cotton swab after 8-h incubation, and then the remaining cells were fixed with formaldehyde and stained with crystal violet for 10 min (Sigma Aldrich, St. Louis, MO, USA). Five fields were randomly selected under an inverted microscope (CX22; Olympus, Tokyo, Japan) to observe and count the cells.

RT-qPCR

Total RNA from exosomes was extracted with Trizol reagent (15596026, Invitrogen, Carlsbad, CA, USA), and first-strand cDNA was synthesized by reverse transcription using an Transcription RT Kit (Tiangen Biotech, Beijing, China). The cDNA was subjected to RT-qPCR using a Fast SYBR Green PCR kit (Applied Biosystems, Foster City, CA, USA) with an ABI PRISM 7300 RT-PCR system (Applied Biosystems). The reaction system was: 95°C for 10 min, followed by 40 cycles at 95°C for 15 s and 60°C for 1 min. Each well was set up with three replicates. Glyceraldehyde 3-phosphate dehydrogenase (GAPDH) was used

as an internal reference to normalize the relative fold change of NEAT1 and ROCK2 expression, and U6 was used as an internal reference to normalize the relative fold change of miR-144-3p expression. Relative RNA levels were analyzed by using the 2^{-ΔΔCt} method and the following equation: $-\Delta\Delta C_t = (\text{average } C_t \text{ value of the target gene in the experimental group} - \text{average } C_t \text{ value of the housekeeper gene in the experimental group}) - (\text{average } C_t \text{ value of the target gene in the control group} - \text{average } C_t \text{ value of the housekeeping gene in the control group})$. RT-qPCR primer design is shown in Table 2.

Western blot

The detailed procedures were based on previous work.³⁰ Cells from each culture group were collected by trypsin digestion, and lysed with an enhanced radio-immunoprecipitation assay (RIPA) lysate containing a protease inhibitor. The protein concentration in cells was then determined using a BCA protein quantification kit. Proteins were also separated by 10% SDS-PAGE. The separated proteins were electro-transferred to a polyvinylidene fluoride (PVDF) membrane and blocked with 5% BSA at room temperature for 2 h to eliminate non-specific binding. Diluted primary antibodies, β-catenin, c-myc, cyclin D1, E-cadherin, and glyceraldehyde-3-phosphate dehydrogenase were added separately and incubated overnight at 4°C. Horseradish peroxidase (HRP)-labeled goat anti-rabbit secondary antibody was added after washing three times and then incubated for 1 h at room temperature. Unbound secondary antibody was removed by washing. The transfer film was then incubated with electrochemiluminescence (ECL) working solution for 1 min at room temperature before imaging. The X-ray film was put in the dark box to expose for 5–10 min to display and fix the image. Image J analysis software was used to quantify the gray levels of each band for protein study. β-actin acted as a loading control for quantitative analysis for each protein of interest, and each protein sample was tested in triplicate.

Dual luciferase analysis

The partial sequences of NEAT1 containing a miR-144-3p binding site and a mutation binding site were amplified by PCR and cloned into a pGL3 promoter vector (Promega, Madison, WI, USA) to construct wild-type (WT) and mutant

Table 2. Primer sequences.

Gene	Primer sequences
NEAT1	F 5'-CTTCCTCCCTTTAACTTATCCATTAC-3'
	R 5'-CTCTTCCTCCACCATTACCAACAATAC-3'
GAPDH	F 5'-GAGCTCAGCTCGCCTGGAGAAAC-3'
	R 5'-TGCTGATCGTAGCCCTTTAGT-3'
miR-144-3p	F 5'- CCTCGCACCTGGAGGCTGGCTG -3'
	R 5'-TTATCAGTTGGGAAAATAGTTA -3'
ROCK2	F 5'-TTACATTGCTATCCACAGAACGG-3'
	R 5'-CTATGCTGCTGCTTTTTGCTC-3'
U6	F 5'- GCAGGAGGTCTTCACAGAG -3'
	R 5'-TCTAGAGGAGAAGCTGGGGT -3'

(MUT) reporter vectors of NEAT1 (NEAT1-WT and NEAT1-MUT). The miR-144-3p mimic or miR-NC and the above-mentioned reporter vector were co-transfected into HEK293 cells using Lipofectamine 3000 (Invitrogen). Luciferase activity was detected using a dual luciferase reporting kit (Beyotim, Beijing, China) after 48 h.

Additionally, the synthetic WT and MUT 3'-untranslated region (UTR) ROCK2 genes were inserted into the pGL3 luciferase reporter vector control vector (Promega, Madison, WI, USA) *via* a targeted binding site (identified using Targetscan) to construct a plasmid. This sequenced luciferase reporter plasmids containing WT and MUT were then co-transfected into HEK293 cells with miR-144-3p mimic or mimic NC, respectively. Cells were collected and lysed after 48 h of transfection, and luciferase activity was detected by using a luciferase detection kit (K801-200, Biovision, Milpitas, CA, USA) with a Glomax 20/20 luminometer fluorescence detector (Promega).

RNA immunoprecipitation analysis

RNA immunoprecipitation (RIP) was performed as previously described with slight modifications.¹⁹ Briefly, CD4⁺T cells were lysed with RIP lysis buffer (Millipore, Billerica, MA, USA). A small portion of the cell lysate was used as a blank negative control (Input), and the remainder of the cell lysate was incubated with Argonaute2 antibody (Anti-Ago2) and immunoglobulin G (IgG) antibody (Anti-IgG) for 1 h at 4°C followed by the

addition of magnetic beads (Millipore) to get the immunoprecipitation complex. The complex was then washed and purified to obtain RNA to remove unbound protein and DNA. Finally, the amount of NEAT1 and miR-144-3p in the purified immunoprecipitation RNA was quantified by RT-qPCR.

RNA pull-down experiment

The RNA pull-down experiment was performed as previously described with minor modifications.^{31,32} Briefly, CD4⁺T cells were transfected with 50 nM of WT biotinylated miR-144-3p and 50 nM of MUT biotinylated miR-144-3p. Cells were collected and washed with PBS after 48 h of transfection. The cells were then incubated with lysis buffer (Ambion, Austin, TX, USA) for 10 min, and the cell lysate was divided into a volumes of 50 µl in each tube for further use. The lysate was incubated with M-280 streptavidin magnetic beads (purchased from Sigma) for 3 h at 4°C, then the immunocomplex was washed successively two times with pre-cold lysis buffer, three times with low salt buffer, and once with high salt buffer. The amount of extracted RNA was quantified by RT-qPCR.

Statistical analysis

Statistical analysis in this study was performed using SPSS 21.0 (IBM, Armonk, NY, USA) statistical software, with $p < 0.05$ taken as statistically significant. Data are shown as the mean \pm standard deviation from independent experiments performed in triplicate. The unpaired *t* test was used

for comparison between two groups. Univariate analysis of variance (ANOVA) was used for multiple group comparisons. Repeated measure ANOVA was used to compare data at various time points. Variables were then analyzed for each experiment.

Results

Serum-derived exosomes of RA patients aggravated the morbidity of CIA mice

Exosomes purified from serum samples were collected from RA patients. The average size of these exosomes (RA-exosomes) was 89.5 nm ($n=10$), which was consistent with the size of exosomes obtained directly from healthy patients (HCs-exosomes, 90 nm) (Figure 1a). TEM images showed that shapes of HCs-exosomes and RA-exosomes were solid and compact, with a typical double-layer membrane structure, and were spherical in shape with a diameter of about 120 nm (Figure 1b). Additionally, the typical exosome markers CD9 and CD63 were identified in our extracted and purified exosomes by western blot; the results demonstrated that, compared with HCs-exosomes, highly expressed CD9 and CD63 were found in RA-exosomes (Figure 1c).

To explore the effects on the mice of exosomes from RA patients, we evaluated five comparative data points in CIA developed mice after they received either 250 ng of human serum-derived exosomes or PBS as placebo treatment on days 25, 30, 35, or 40. The results showed that the incidence of RA appeared more apparent and more frequent in exosome-injected CIA mice compared with those with PBS treatment (Figure 1d). The clinical score for arthritis in mice dramatically increased after exosomes injection (Figure 1e). CT imaging and histomorphometry analysis revealed higher bone surface erosion (identified by the ratio of area/volume) and lower bone thickness in the exosomes injected group, indicating the deterioration of the bone structures (Figure 1f–h). The aforementioned findings clarified a promotive role of RA exosomes in RA occurrence.

Effects of serum-derived exosomes from patients with RA on proliferation and apoptosis of CD4⁺T cells and Th17 differentiation

Considering the role of cellular immune function in RA patients and the differentiation of CD4⁺T cells into Th17 cells for the development of

RA,^{14,24,26} the effects of the serum-derived exosomes of RA patients on CD4⁺T cell proliferation, apoptosis, and Th17 differentiation were analyzed. The result indicated that serum-derived exosomes from RA patients promoted proliferation of CD4⁺T cells (Figure 2a) and inhibited CD4⁺T cell apoptosis in RA patients (Figure 2b). Besides, these exosomes also promoted CD4⁺T cell differentiation to Th17 cells (Figure 2c and Supplemental Figure S1a), and support CCL20-mediated Th17 chemotaxis in RA patients (Figure 2d). Thus, serum-derived exosomes could promote CD4⁺T cell proliferation and differentiation.

Increased expression of NEAT1 in serum-derived exosomes of RA patients

Studies have shown that the functions of extracellular vesicles such as exosomes are considerably diverse, and are characterized by intercellular communication through the transmission of proteins, mRNA, miRNA, and lncRNAs.²⁷ As a crucial regulator of pathological changes, the role of exosomal lncRNA was further studied in patients suffering from RA. In our work, new insights into NEAT1 expression were clinically evaluated. Our results indicate an obviously enhanced expression of NEAT1 in the exosomes of RA patients compared with those from healthy controls (Figure 3a). NEAT1 expression was also upregulated in the CD4⁺T cells after being incubated with serum-derived exosomes of RA patients (Figure 3b).

Binding of NEAT1 to miR-144-3p

To further understand the mechanism of the action of NEAT1 in CD4⁺T cells, StarBase was used for bioinformatics analysis. NEAT1 and miR-144-3p had complementary binding sites, as shown in Figure 4a. Additionally, the expression of miR-144-3p in CD4⁺T cells was significantly upregulated by knocking down the NEAT1 gene by sh-NEAT1 (Figure 4b). Treatment with a negative control of NEAT1, sh-NC, resulted in a relatively low expression of miR-144-3p, suggesting an inverse correlation between NEAT1 and miR-144-3p (Figure 4b). Next, the dual luciferase reporter method, RIP, and RNA pull-down experiments were used to explore whether NEAT1 acted as competing endogenous RNA (ceRNA) to mediate miR-144-3p expression in CD4⁺T cells. The dual luciferase report test showed that addition of the miR-144-3p mimic significantly suppressed the

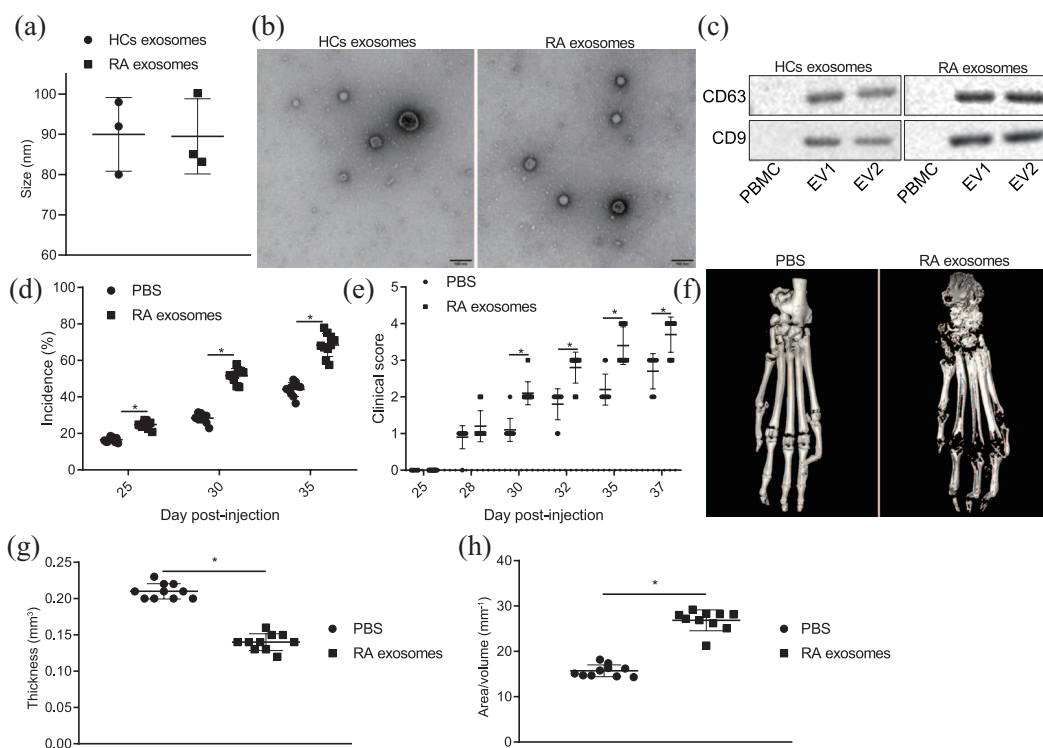


Figure 1. Promotive effects of the serum-derived exosomes of RA patients on CIA mice. (a) Size distribution of purified exosomes presented in RA patients. (b) Morphology of purified exosomes presented in RA patients. (c) Western blot results of common exosome markers CD9 and CD63. PBMC and exosome samples (EV1 and EV2) were collected from RA patients or healthy controls. (a–c) Each sample was analyzed three times. (d) Morbidity rate of CIA mice at various time point after exosome injection ($n=10$). (e) Clinical scores for PBS- or exosome-treated CIA mice ($n=10$). (f) Typical 3D reconstructed image of the hind paw in PBS- or exosome-treated group ($n=5$). (g) Average thickness of the wedge-shaped bone at the hind paw of CIA mice ($n=10$). (h) Average bone degradation of the wedge-shaped bone ($n=10$). Data expressed as mean \pm SD, data were compared between the two groups using unpaired t test. * $p < 0.05$.

CIA, collagen-induced arthritis; 3D, three-dimensional; PBMC, peripheral blood mononuclear cell; PBS, phosphate-buffered saline; RA, rheumatoid arthritis; SD, standard deviation.

luciferase activity of NEAT1 normal type reporter vectors (NEAT1-WT), whereas it did not affect the luciferase activity of the mutated vectors (NEAT1-MUT) (Figure 4c). Both NEAT1 and miR-144-3p were detected and expressed *via* Ago2 immunoprecipitation since Ago2 is a key catalytic component of the RNA containing RNA-induced silencing complex (RISC). RIP analysis demonstrated that NEAT1 and miR-144-3p were detected in the control group (shown as anti-NC) (Figure 4d). Compared with the control group, the amount of purified NEAT1 from cells treated with miR-144-3p inhibitor was drastically reduced, whereas the levels of miR-144-3p was not changed significantly (Figure 4d), indicating that NEAT1 may be present in the miR-144-3p, which combined with the Ago2-RISC complex. The RNA pull-down

experiment indicated that NEAT1 was pulled down by miR-144-3p, while miR-144-3p-MUT with a mutation failed to bind with and pull down NEAT1 (Figure 4e), revealing that miR-144-3p had a negative effect on NEAT1 in terms of sequence specific recognition. In summary, our results proved that miR-144-3p can bind NEAT1.

NEAT1 promotes expression of ROCK2 through miR-144-3p

NEAT1 regulated miR-144-3p in CD4⁺T cells, and NEAT1 might regulate the target gene of miR-144-3p by acting as ceRNA. Gene silencing of NEAT1 (sh-NEAT1) suppressed transcription of the *ROCK2* gene in CD4⁺T cells (Figure 5a), which is consistent with western blot results

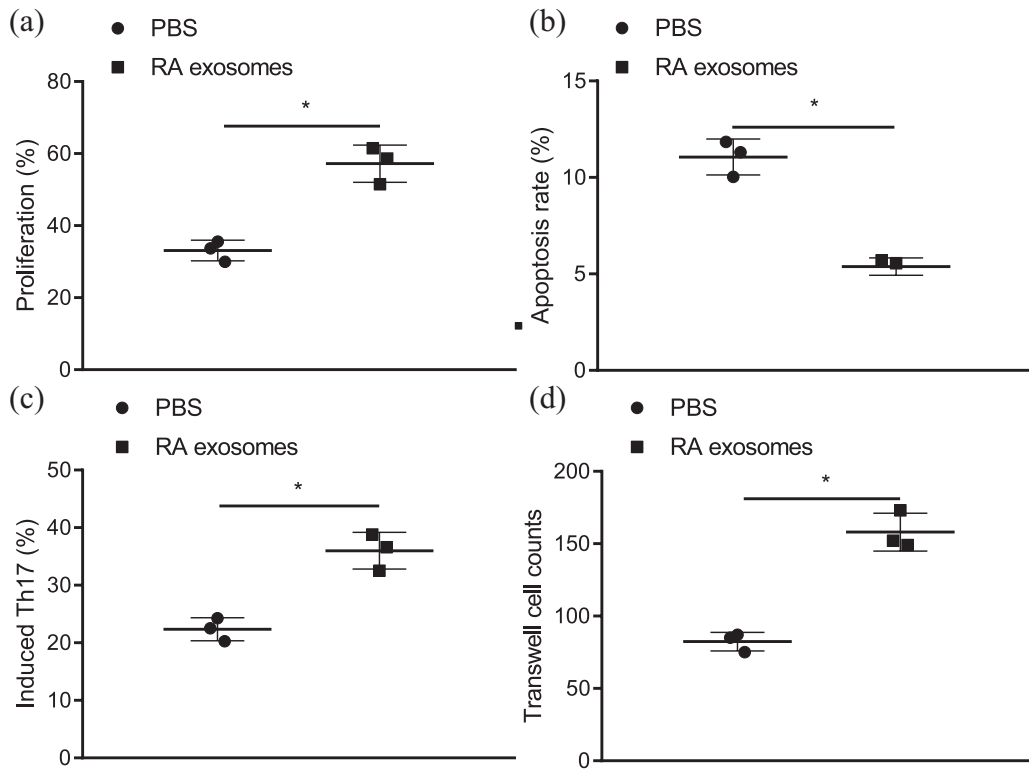


Figure 2. The effect of serum-derived exosomes of RA patients on CD4⁺T cells proliferation, apoptosis, and Th17 cell differentiation. (a) CD4⁺T cell proliferation study after 5 days of exosomes treatment ($n=3$). (b) CD4⁺T cell apoptosis study after 5 days of exosomes treatment ($n=3$). (c) Flow cytometry results for Th17 cell differentiation after applying serum-derived exosomes of RA patients ($n=3$). (d) CCL20-mediated Th17 chemotaxis ($n=3$). Data are expressed as mean \pm SD, data comparison between groups was by unpaired t test. $*p < 0.05$.

PBS, phosphate-buffered saline; RA, rheumatoid arthritis; SD, standard deviation.

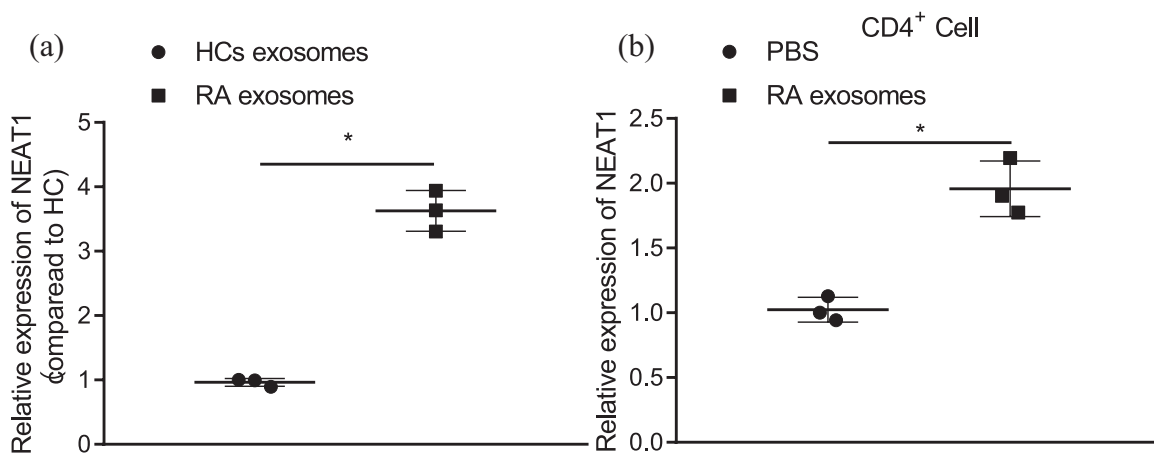


Figure 3. Increased expression of NEAT1 in serum-derived exosomes of RA patients. (a) RT-qPCR result of the expression of NEAT1 in exosomes of RA patients (RA, $n=68$; HC, $n=20$). (b) RT-qPCR result of the expression of NEAT1 in CD4⁺T cells after being incubated with serum-derived exosomes of RA patients ($n=3$). Data are expressed as mean \pm SD, data comparison between groups was by unpaired t test. $*p < 0.05$.

HC, healthy control; NEAT1, nuclear enriched abundant transcript 1; PBS, phosphate-buffered saline; RA, rheumatoid arthritis; RT-qPCR, reverse transcription-quantitative polymerase chain reaction; SD, standard deviation.

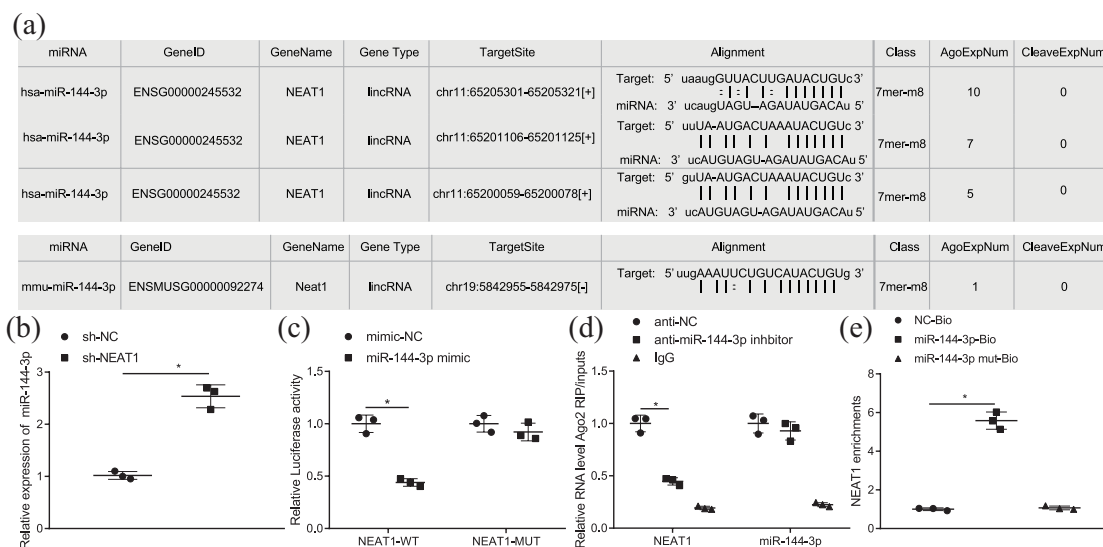


Figure 4. Binding of NEAT1 to miR-144-3p. (a) Binding site between NEAT1 and miR-144-3p. (b) RT-qPCR data for miR-144-3p expression under sh-NEAT1 or sh-NC treatment in CD4⁺T cells ($n=3$). (c) Luciferase activity of NEAT1-WT/MUT after addition of miR-144-3p mimic in CD4⁺T cells ($n=3$). (d) Physical association between NEAT1 and miR-144-3p. Expression of NEAT1 and miR-144-3p were detected by RIP assay and described using the level of Ago2. (e) Pull-down experiment result of CD4⁺T cells transfected with miR-144-3p-Bio, miR-144-3p-Mut-Bio, or NC-Bio for 48 h ($n=3$). Data are expressed as mean \pm SD, data comparison between two groups was by unpaired t test, single-factor ANOVA was used for comparison between multiple groups. * $p < 0.05$, ** $p < 0.01$.

ANOVA, analysis of variance; miR-144-3p-Bio, biotinylated WT miR-144-3p; miR-144-3p-Mut-Bio, biotinylated mutant miR-144-3p; MUT, mutant; NC-Bio, biotinylated NC; NEAT1, nuclear enriched abundant transcript 1; RIP, RNA immunoprecipitation; RT-qPCR, reverse transcription-quantitative polymerase chain reaction; SD, standard deviation; sh-NEAT1, shRNA targeting NEAT1; sh-NC, shRNA negative control; WT, wild type.

(Figure 5b, c). To prove the relationship between miR144-3p and ROCK2 in cells, miR-144-3p mimic transfection was used to enhance expression of miR-144-3p in CD4⁺T cells, and expression of ROCK2 was detected by RT-qPCR and western blotting, respectively. RT-qPCR results suggested that *ROCK2* gene transcription in the miR-144-3p mimic group was significantly less than in the control group (Figure 5d). The same results were also observed in the western blot study (Figure 5e). To verify that ROCK2 expression was affected by miR-144-3p *via* binding to its 3'-UTR site, a dual luciferase activity assay was performed to evaluate the binding ability of miR-144-3p towards ROCK2. Wild-type ROCK2 (WT-ROCK2) and mutant (MUT-ROCK2) sequences were designed as shown in Figure 5f. The measurements of dual luciferase activity showed that the luciferase activity measured after miR-144-3p mimic transfection was lower than that with negative controls in the WT-ROCK2 group. However, the MUT-ROCK2 group exhibited no difference between the miR-144-3p mimic

group and negative controls (Figure 5g). We concluded that miR144-3p could directly bind the 3'-UTR region of ROCK2, and NEAT1 might act as a ceRNA to increase expression of the miR144-3p-targeted gene *ROCK2*.

Effects of NEAT1-miR-144-3p-ROCK2 axis on CD4⁺T cell proliferation, apoptosis, and Th17 cell differentiation

In our research, we further performed a flow cytometry study to explore whether the NEAT1-miR-144-3p-ROCK2 axis exerts an influence on CD4⁺T cell proliferation, apoptosis, and Th17 cells differentiation. Knockout of NEAT1 gene or the addition of miR-144-3p limited CD4⁺T cell proliferation and stimulated the CD4⁺T cell apoptosis process. The inclusion of either miR-144-3p inhibitor or ROCK2 after silencing NEAT1 reversed the outcomes listed above and indicated their potential to control the loss or demolition of CD4⁺T cells (Figure 6a,b). Additionally, knock-down of NEAT1 or treatment with miR-144-3p

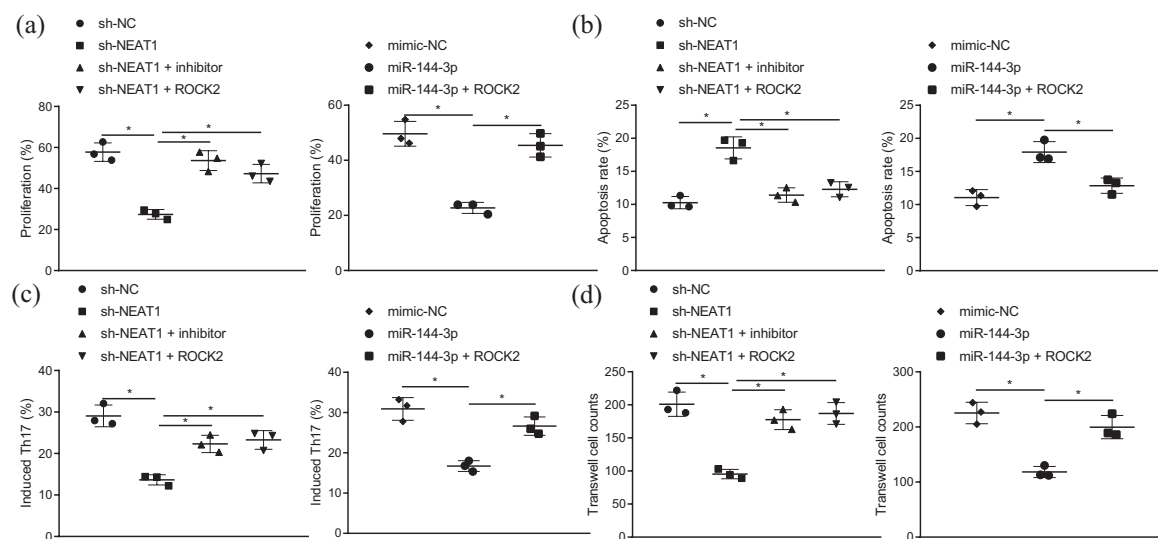


Figure 6. Effect of the NEAT1-miR-144-3p-ROCK2 axis on CD4⁺T cell proliferation, apoptosis, and Th17 differentiation. (a) Cell proliferation study with silenced NEAT1, miR-144-3p, miR-144-3p inhibitor, and ROCK2 ($n=3$). Sorted CD4⁺ T cells were stained with 5 μ M CFSE and stimulated with anti-CD3 and anti-CD28 mAbs. (b) Flow cytometry was applied for cell apoptosis study ($n=3$). (c) CD4⁺ T cells were transfected before Th17 cell differentiation, and the percentage of Th17 cells was analyzed by flow cytometry. (d) Transwell analysis for Th17 cell chemotaxis ($n=3$). Data are expressed as mean \pm SD; data comparison between the two groups was using unpaired t test.

* $p < 0.05$.

CFSE, 5(6)-carboxyfluorescein diacetate succinimidyl ester; mAbs, monoclonal antibodies; NEAT1, nuclear enriched abundant transcript 1; ROCK2, Rho-associated protein kinase 2; SD, standard deviation.

(Figure 7d). Therefore, NEAT1 gene might promote the progress of RA *via* the ROCK2-associated WNT signaling pathway.

Inhibition of NEAT1 alleviated CIA in mice

Further *in vivo* assays were performed. We found that CIA mice had increased clinical scores of RA, and addition of sh-NEAT1 decreased the clinical scores significantly (Figure 8a). After observation through CT imaging, the bone surface erosion and bone degradation of CIA mice were significantly higher than that of the control group, while the addition of sh-NEAT1 significantly improved the above conditions (Figure 8b–d). At 37 days after immunization, flow cytometry analysis showed that expression of IL-17A in the joint tissues of CIA mice increased by about three times, while expression of IL-17A in the joint tissues of CIA mice with downregulated NEAT1 was significantly lower than that of CIA mice with sh-NC (Figure 8e and Supplemental Figure S1c). Our data demonstrate that knocking down NEAT1 could improve RA symptoms in CIA mice, accompanied by a decrease in IL-17 expression.

The expression of NEAT1, miR-144-3p, and ROCK2 in joint tissues was determined through RT-qPCR and the results revealed that CIA mice had elevated NEAT1 and ROCK2 expression but reduced miR-144-3p expression; the addition of sh-NEAT1 led to opposite trends (Figure 8f). Besides, western blot analysis showed that CIA mice had elevated ROCK2, β -catenin, c-myc, and cyclin D1 expression, but decreased E-cadherin expression; the addition of sh-NEAT1 led to opposite trends (Figure 8g).

Discussion

There are a number of important findings in this study. First, we found that exosome treatment increased the chance of developing RA in animals. Exosomes also increased CD4⁺T cell differentiation to Th17, which is an important process for the development of RA. Second, NEAT1 expression was increased in RA. NEAT1 was found to bind to, and inhibit the expression of, miR-144-3p. NEAT1 increased the expression of ROCK2 by inhibiting miR-144-3p. Third, NEAT knockdown or miR-144-3p overexpression decreased CD4⁺T

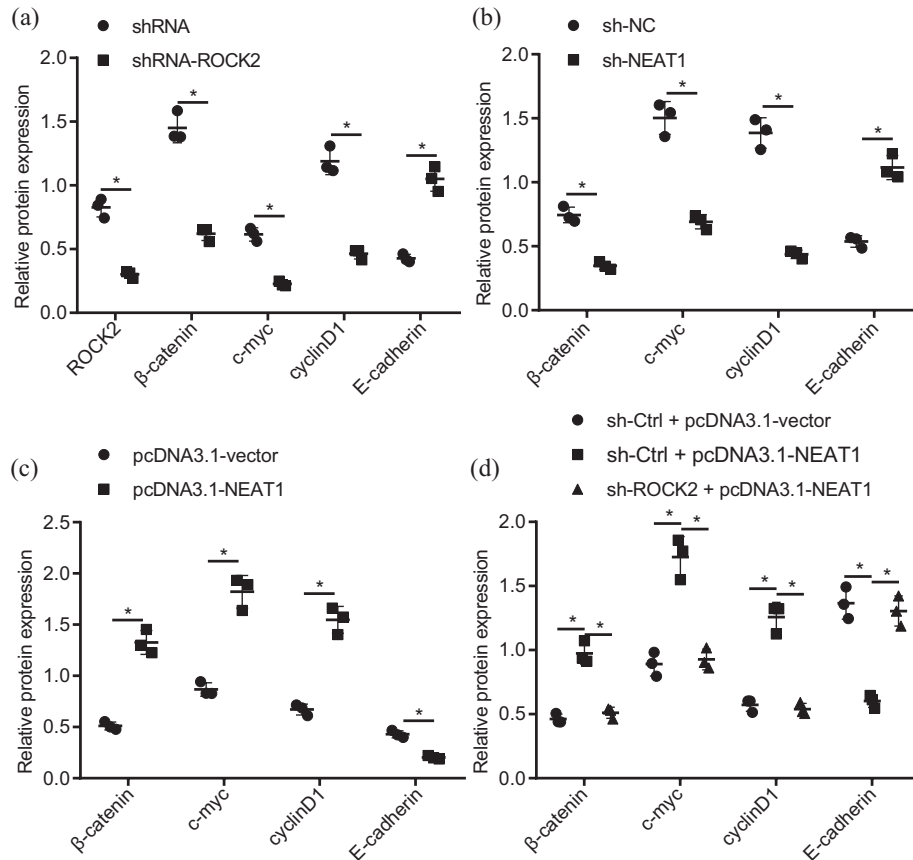


Figure 7. NEAT1 promotes the progression of RA through the WNT signaling pathway. (a) Westerns blot result of the ROCK, β -catenin, c-myc, cyclin D1, and E-cadherin after CD4⁺T cells were transfected with shRNA-ROCK2 for 48 h ($n=3$). (b) Western blot results of the β -catenin, c-myc, cyclin D1, and E-cadherin after CD4⁺T cells were transfected with sh-NEAT1 or sh-NC for 48 h ($n=3$). (c) Western blot results of the expression of β -catenin, c-myc, cyclin D1, and E-cadherin after overexpressing NEAT1 ($n=3$). (d) Overexpression of NEAT1 promoted the WNT signaling pathway to restore the function of siRNA-ROCK2 ($n=3$). Data are expressed as mean \pm SD; data comparison between the two groups was using unpaired *t* test.

* $p < 0.05$.

NEAT1, nuclear enriched abundant transcript 1; RA, rheumatoid arthritis; ROCK2, Rho-associated protein kinase 2; SD, standard deviation.

cell proliferation and increased apoptosis. Fourth, NEAT1 knockdown also decreased important mediators in the Wnt/ β -catenin pathway. These results collectively suggest that NEAT1 inhibited miR-144-3p, upregulated ROCK2 and activated Wnt/ β -catenin pathway, leading to promoted the progression of RA. These mediators, such as the inhibition of NEAT1, may be a potential strategy for RA treatment.

Mortality of RA remains on an upward trend.⁵ Although RA affects only about 1% of the population, it remains a common autoimmune disorder that can cause decreased mobility and disability.^{1,3} Treatment remains unsatisfactory, probably because of the complexity of the disease and

incomplete understanding of the underlying mechanism. In this study, exposure to exosome increased RA progression, as shown by increased CD4⁺T cell differentiation to Th17 cells. This process is critical for RA progression.^{11,12} The functions of extracellular vesicles are diverse, including intercellular communications through a wide variety of molecules including lncRNAs.¹³ Our results, therefore, suggest that a molecule in extracellular vesicles is critical to the progression of RA.

As we continued to examine the molecular mechanisms of RA, we found that NEAT1 was upregulated in RA. This result is comparable with that from a previous study that showed upregulated NEAT1 in blood from patients with RA.¹⁶

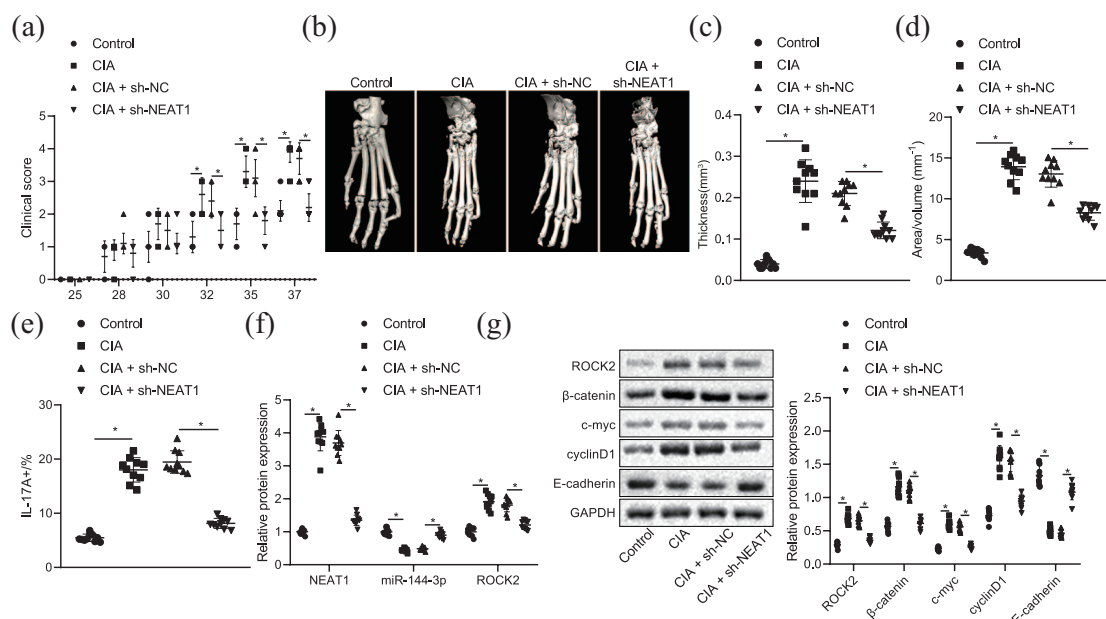


Figure 8. Inhibition of NEAT1 alleviated CIA in mice. (a) Clinical scores of mice in different groups ($n = 10$). (b) Typical 3D reconstruction image of hind paw ($n = 5$). (c) Evaluation of the average thickness of mouse wedge-shaped bones with histomorphometric μ CT analysis. (d) Evaluation of the average bone degradation of wedge-shaped bones with area/volume parameters ($n = 10$). (e) Flow cytometric analysis of IL-17A expression in joint tissues ($n = 10$). (f) Expression of NEAT1, miR-144-3p and ROCK2 in joint tissues was determined through RT-qPCR ($n = 10$). (g) Western blot analysis of protein levels of ROCK2, β -catenin, c-myc, cyclin D1, and E-cadherin ($n = 10$). Data are expressed as mean \pm SD; data comparison between the two groups was using unpaired t test. $*p < 0.05$.

CIA, collagen-induced arthritis; μ CT microcomputer computed tomography, 3D, three-dimensional; NEAT1, nuclear enriched abundant transcript 1; ROCK2, Rho-associated protein kinase 2; RT-qPCR, reverse transcription-quantitative polymerase chain reaction; SD, standard deviation.

NEAT1 has also been shown to be linked to RA through the signaling molecule STAT1.^{33,34} Results from our study, however, suggest that NEAT1 may be involved in another, STAT1-independent, pathway.

Another important finding is that NEAT1 bound and inhibited the expression of miR-144-3p. This result agrees with two previous studies showing that miR-144-3p is involved in RA and is bound by NEAT1.^{18,19} How miR-144-3p is involved in RA remains to be determined, but our study showed that miR-144-3p overexpression reduced CD4⁺T cells proliferation and increased their apoptosis. miR-144-3p overexpression also reduced ROCK2 expression. Moreover, miR-144-3p has also been shown previously to regulate immune response and inflammation.^{35,36} These results suggest that miR-144-3p may have anti-RA characteristics.

We also found that miR-144-3p was linked to the activation of ROCK2 in RA, which is in line with

previous studies.^{20,21} Furthermore, upregulation of ROCK2 led to upregulation of Wnt/ β -catenin. This result is comparable with previous findings that ROCK2 activates Wnt/ β -catenin signaling pathway, which is involved in RA.^{23,24} Downstream pathway of Wnt/ β -catenin may include tumor necrosis factor α in RA.²⁵

In conclusion, we found that NEAT1 inhibits miR-144-3p, leading to activation of the ROCK2 and Wnt/ β -catenin signaling pathway, resulting in the progression of RA (Figure 9). However, RA is a complicated disease that includes autoimmune and inflammation components. Animal models of RA include, but are not limited to, collagen-induced, adjuvant-induced, antibody-induced, and genetically altered (tumor necrosis factor α overexpression) models.^{37,38} Each animal model mimics several properties of the human disease. In this study, we used only one model, and, therefore, the results of this study should be confirmed in other animal models.

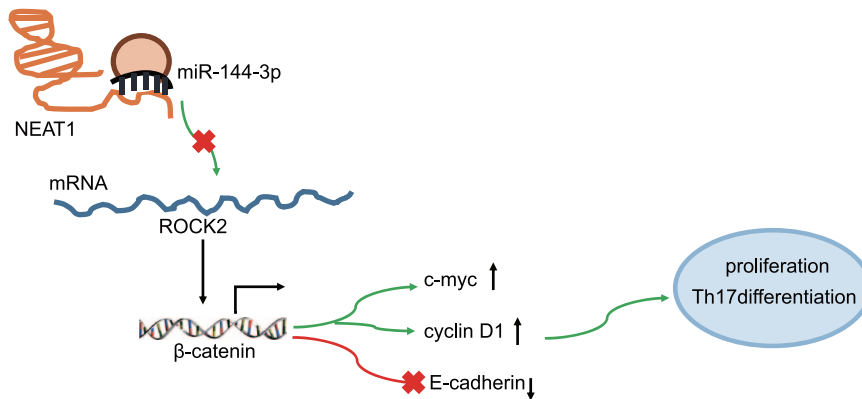


Figure 9. Mechanistic diagram of lncRNA NEAT1 in blood exosomes of RA patients promoting the occurrence of RA by mediating the miR-144-3p/ROCK2 axis to regulate the WNT signaling pathway. lncRNA NEAT1 acts as a ceRNA to mediate miR-144-3p expression in CD4⁺T cells; thereby, NEAT1 promotes expression of ROCK2. Expression of c-myc and cyclin D1 is then increased significantly, while expression of E-cadherin is increased significantly. NEAT1, miR-144-3p inhibitor, and ROCK2 support CD4⁺T cell proliferation and Th17 differentiation, but limit CD4⁺T cell apoptosis.

ceRNA competing endogenous RNA, lncRNA, long noncoding RNA; NEAT1, nuclear enriched abundant transcript 1; RA, rheumatoid arthritis; ROCK2, Rho-associated protein kinase 2.

Acknowledgements

We acknowledge and appreciate our colleagues for their valuable efforts and comments on this paper.

Author contributions

RL and CBJ conceived and designed the research. JJL and XRL performed experiments. LZ and HFY analyzed data. WWX interpreted results of experiments. WJF prepared figures. QHL and HLD drafted manuscript. RL and CBJ edited and revised manuscript. All authors approved final version of manuscript.

Conflict of interest statement

The authors declare that there is no conflict of interest.


Ethical statement

All study participants signed informed consent to provide peripheral blood for the study. The research was approved by the Ethics committee of Suzhou Traditional Chinese Medicine Hospital Affiliated to Nanjing University of Chinese Medicine and all operations were in compliance with the Declaration of Helsinki. The All animal experiments were performed with the approval from the institutional animal care and use committee of Suzhou Traditional Chinese Medicine Hospital Affiliated to Nanjing University of Chinese Medicine hospital.

Funding

The authors disclosed receipt of the following financial support for the research, authorship, and/or publication of this article: This work was supported by the Science and Technology Project of Suzhou City of China (No. SYS2019109).

ORCID iD

Qihong Liu  <https://orcid.org/0000-0002-2728-3907>

Supplemental material

Supplemental material for this article is available online.

References

1. van der Woude D and van der Helm-van Mil AHM. Update on the epidemiology, risk factors, and disease outcomes of rheumatoid arthritis. *Best Pract Res Clin Rheumatol* 2018; 32: 174–187.
2. Gibofsky A. Epidemiology, pathophysiology, and diagnosis of rheumatoid arthritis: a synopsis. *Am J Manag Care* 2014; 20: S128–S135.
3. Smolen JS, Aletaha D and McInnes IB. Rheumatoid arthritis. *Lancet* 2016; 388: 2023–2038.
4. Ngian GS. Rheumatoid arthritis. *Aust Fam Physician* 2010; 39: 626–628.

5. Myasoedova E, Davis JM III, Crowson CS, *et al.* Epidemiology of rheumatoid arthritis: rheumatoid arthritis and mortality. *Curr Rheumatol Rep* 2010; 12: 379–385.
6. De Cock D and Hyrich K. Malignancy and rheumatoid arthritis: epidemiology, risk factors and management. *Best Pract Res Clin Rheumatol* 2018; 32: 869–886.
7. Scott DL, Wolfe F and Huizinga TW. Rheumatoid arthritis. *Lancet* 2010; 376: 1094–1108.
8. Alarcon GS. Epidemiology of rheumatoid arthritis. *Rheum Dis Clin North Am* 1995; 21: 589–604.
9. Korani S, Korani M, Butler AE, *et al.* Genetics and rheumatoid arthritis susceptibility in Iran. *J Cell Physiol* 2019; 234: 5578–5587.
10. Kondo Y, Yokosawa M, Kaneko S, *et al.* Review: transcriptional regulation of CD4⁺ T cell differentiation in experimentally induced arthritis and rheumatoid arthritis. *Arthritis Rheumatol* 2018; 70: 653–661.
11. Komatsu N, Okamoto K, Sawa S, *et al.* Pathogenic conversion of Foxp3⁺ T cells into TH17 cells in autoimmune arthritis. *Nat Med* 2014; 20: 62–68.
12. Zhang Y, Li Y, Lv TT, *et al.* Elevated circulating Th17 and follicular helper CD4⁺ T cells in patients with rheumatoid arthritis. *APMIS* 2015; 123: 659–666.
13. van Niel G, D'Angelo G and Raposo G. Shedding light on the cell biology of extracellular vesicles. *Nat Rev Mol Cell Biol* 2018; 19: 213–228.
14. Raposo G and Stoorvogel W. Extracellular vesicles: exosomes, microvesicles, and friends. *J Cell Biol* 2013; 200: 373–383.
15. Beer L, Zimmermann M, Mitterbauer A, *et al.* Analysis of the secretome of apoptotic peripheral blood mononuclear cells: impact of released proteins and exosomes for tissue regeneration. *Sci Rep* 2015; 5: 16662.
16. Song J, Kim D, Han J, *et al.* PBMC and exosome-derived Hotair is a critical regulator and potent marker for rheumatoid arthritis. *Clin Exp Med* 2015; 15: 121–126.
17. Liu H, Hu PW, Couturier J, *et al.* HIV-1 replication in CD4⁺ T cells exploits the down-regulation of antiviral NEAT1 long non-coding RNAs following T cell activation. *Virology* 2018; 522: 193–198.
18. Zhao C, Li X, Yang Y, *et al.* An analysis of Treg/Th17 cells imbalance associated microRNA networks regulated by moxibustion therapy on Zusanli (ST36) and Shenshu (BL23) in mice with collagen induced arthritis. *Am J Transl Res* 2019; 11: 4029–4045.
19. Wei JL, Wu CJ, Chen JJ, *et al.* LncRNA NEAT1 promotes the progression of sepsis-induced myocardial cell injury by sponging miR-144-3p. *Eur Rev Med Pharmacol Sci* 2020; 24: 851–861.
20. Wang Y, Zhang Y, Yang T, *et al.* Long non-coding RNA MALAT1 for promoting metastasis and proliferation by acting as a ceRNA of miR-144-3p in osteosarcoma cells. *Oncotarget* 2017; 8: 59417–59434.
21. Zanin-Zhorov A, Weiss JM, Nyuydzefe MS, *et al.* Selective oral ROCK2 inhibitor down-regulates IL-21 and IL-17 secretion in human T cells via STAT3-dependent mechanism. *Proc Natl Acad Sci U S A* 2014; 111: 16814–16819.
22. Weng CH, Gupta S, Geraghty P, *et al.* Cigarette smoke inhibits ROCK2 activation in T cells and modulates IL-22 production. *Mol Immunol* 2016; 71: 115–122.
23. Luo J, Lou Z and Zheng J. Targeted regulation by ROCK2 on bladder carcinoma via Wnt signaling under hypoxia. *Cancer Biomark* 2019; 24: 109–116.
24. Ma B and Hottiger MO. Crosstalk between Wnt/ β -catenin and NF- κ B signaling pathway during inflammation. *Front Immunol* 2016; 7: 378.
25. Li Y, Yuan L, Jiang S, *et al.* Interleukin-35 stimulates tumor necrosis factor- α activated osteoblasts differentiation through Wnt/ β -catenin signaling pathway in rheumatoid arthritis. *Int Immunopharmacol* 2019; 75: 105810.
26. Yolbas S, Yildirim A, Tektemur A, *et al.* Paricalcitol inhibits the Wnt/ β -catenin signaling pathway and ameliorates experimentally induced arthritis. *Turk J Med Sci* 2018; 48: 1080–1086.
27. Wang L, Wang C, Jia X, *et al.* Circulating exosomal miR-17 inhibits the induction of regulatory T cells via suppressing TGFBR II expression in rheumatoid arthritis. *Cell Physiol Biochem* 2018; 50: 1754–1763.
28. Cosenza S, Toupet K, Maumus M, *et al.* Mesenchymal stem cells-derived exosomes are more immunosuppressive than microparticles in inflammatory arthritis. *Theranostics* 2018; 8: 1399–1410.
29. Ren Y, Yang B, Yin Y, *et al.* Aberrant CD200/CD200R1 expression and its potential role in Th17 cell differentiation, chemotaxis and

- osteoclastogenesis in rheumatoid arthritis. *Rheumatology (Oxford)* 2015; 54: 712–721.
30. Luo Y, Chen JJ, Lv Q, *et al.* Long non-coding RNA NEAT1 promotes colorectal cancer progression by competitively binding miR-34a with SIRT1 and enhancing the Wnt/ β -catenin signaling pathway. *Cancer Lett* 2019; 440–441: 11–22.
31. Lal A, Thomas MP, Altschuler G, *et al.* Capture of microRNA-bound mRNAs identifies the tumor suppressor miR-34a as a regulator of growth factor signaling. *PLoS Genet* 2011; 7: e1002363.
32. Wang H, Huo X, Yang XR, *et al.* STAT3-mediated upregulation of lncRNA HOXD-AS1 as a ceRNA facilitates liver cancer metastasis by regulating SOX4. *Mol Cancer* 2017; 16: 136.
33. Mishra S, Verma SS, Rai V, *et al.* Long non-coding RNAs are emerging targets of phytochemicals for cancer and other chronic diseases. *Cell Mol Life Sci* 2019; 76: 1947–1966.
34. Shui X, Chen S, Lin J, *et al.* Knockdown of lncRNA NEAT1 inhibits Th17/CD4⁺ T cell differentiation through reducing the STAT3 protein level. *J Cell Physiol* 2019; 234: 22477–22484.
35. Sun G, Lu Y, Zhao L, *et al.* Hemin impairs resolution of inflammation via microRNA-144-3p-dependent downregulation of ALX/FPR2. *Transfusion* 2019; 59: 196–206.
36. Liu J, Liu J, Xiao L, *et al.* Identification of differentially expressed miRNAs in the response of spleen CD4⁺ T cells to electroacupuncture in senescence-accelerated mice. *Cell Biochem Biophys* 2020; 78: 89–100.
37. Choudhary N, Bhatt LK and Prabhavalkar KS. Experimental animal models for rheumatoid arthritis. *Immunopharmacol Immunotoxicol* 2018; 40: 193–200.
38. Caplazi P, Baca M, Barck K, *et al.* Mouse models of rheumatoid arthritis. *Vet Pathol* 2015; 52: 819–826.

Visit SAGE journals online
[journals.sagepub.com/
home/taj](https://journals.sagepub.com/home/taj)

 SAGE journals